

Constraints on diffuse gamma-ray emission from structure formation processes in the Coma cluster

Fabio Zandanel* and Shin'ichiro Ando†

GRAPPA Institute, University of Amsterdam, 1098XH Amsterdam, Netherlands

10 July 2018

ABSTRACT

We analyze 5-year (63 months) data of the Large Area Telescope on board *Fermi* satellite from the Coma galaxy cluster in the energy range between 100 MeV and 100 GeV. The likelihood analyses are performed with several templates motivated by models predicting gamma-ray emission due to structure formation processes. We find no excess emission and derive the most stringent constraints to date on the Coma cluster above 100 MeV, and on the tested scenarios in general. The upper limits on the integral flux range from 10^{-10} to 10^{-9} $\text{cm}^{-2} \text{s}^{-1}$, and are stringent enough to challenge different scenarios. We find that the acceleration efficiency of cosmic ray protons and electrons at shocks must be below approximately 15% and 1%, respectively. Additionally, we argue that the proton acceleration efficiency should be lower than 5% in order to be consistent with radio data. This, however, relies on magnetic field estimates in the cluster. In particular, this implies that the contribution to the diffuse extragalactic gamma-ray background due to gamma-rays from structure formation processes in clusters of galaxies is negligible, below 1%. Finally, we discuss future detectability prospects for Astro-H, *Fermi* after 10-yr of operation, and the Cherenkov Telescope Array.

Key words: Galaxies: gamma-rays: galaxies: clusters — galaxies: clusters: individual: Coma

1 INTRODUCTION

According to the hierarchical scenario, structures form via accretion and merger of smaller objects into larger ones. Clusters of galaxies are the latest and largest structures to have formed in the Universe. They have typical radii of a few Mpc, and masses of about 10^{14} – $10^{15} M_{\odot}$. Dark matter contributes for about 80% of their mass, gas for 15% and galaxies for 5% (Voit 2005). During the course of a cluster formation, part of its gravitational binding energy, on the order of 10^{61} – 10^{63} erg, should be dissipated through turbulence and structure-formation (accretion and merger) shocks that accelerate charged particles such as protons and electrons. Even if only a small fraction of this energy goes into the particle acceleration, the process should be strong enough to make the clusters visible with non-thermal emissions such as radio synchrotron emission, and potentially in gamma-ray frequencies.

Diffuse radio synchrotron emission is detected in the Coma cluster both as a central radio *halo* and as a peripheral radio *relic* (e.g., Deiss et al. 1997; Brown & Rudnick 2011).

This proves the presence of relativistic electrons and magnetic fields permeating the intra-cluster medium (ICM). Radio relics are apparently connected to structure-formation shocks (e.g., van Weeren et al. 2011), even though the details of the particle acceleration process at place are not clear yet (e.g., Ogreshnikov et al. 2013; Pinzke et al. 2013). Radio halos can be further divided into two categories: mini-halos and giant halos. The former is associated with relaxed, cool-core clusters, and typically extend over a few hundred kpc. The latter, such as the one found in Coma, is typically associated with cluster mergers and have Mpc-sizes (see Feretti et al. 2012, for a review). The generation mechanism of radio halos is currently debated between re-acceleration (e.g., Brunetti & Lazarian 2007, 2011; Brunetti et al. 2012) and hadronic models (e.g., Pfrommer & Enßlin 2004a,b; Pfrommer et al. 2008; Enßlin et al. 2011; Zandanel et al. 2014b).

Cosmic ray (CR) electrons can generate X-ray and gamma-ray emission through inverse Compton (IC) up-scattering of cosmic-microwave-background (CMB) photons. Additionally, if the radio emission is due to secondary electrons generated in hadronic interactions between CR protons and the ICM, it should be accompanied by a de-

* f.zandanel@uva.nl

† s.ando@uva.nl

tectable gamma-ray emission generated from neutral pion decays.

Observationally, gamma-ray emission from clusters of galaxies were searched for the last several years to decade, but all these attempts resulted in no detection (for space-based cluster observations in the GeV-band, see Reimer et al. 2003; Fermi-LAT Collaboration 2010a,b; Zimmer et al. 2012; Han et al. 2012; Ando & Nagai 2012; Huber et al. 2013; for ground-based observations in the energy band above ~ 100 GeV, see Perkins et al. 2006; Perkins 2008; HESS Collaboration 2009a,b; Domainko et al. 2009; Galante et al. 2009; Kiuchi et al. 2009; VERITAS Collaboration 2009; MAGIC Collaboration 2010, 2012; VERITAS Collaboration 2012; HESS Collaboration 2012). Recently, both Fermi-LAT Collaboration (2013) and Prokhorov & Churazov (2013) performed a joint likelihood analysis of about 50 galaxy clusters. They found a significant gamma-ray excess in the direction of few objects, particularly Abell 400, which however is interpreted either as coming from active galactic nuclei (AGN) within the cluster or as un-modeled background.

The Large Area Telescope (LAT) on board *Fermi* satellite¹ continuously surveys the gamma-ray sky since August 2008, and its data represent a unique tool to test diffuse CR emission models in clusters of galaxies. Although many previous analyses of the *Fermi*-LAT data of galaxy clusters were based on the assumption that the clusters were simply point sources or have a very simple extended profile, a possible cluster gamma-ray emission could have very different spatial structure compared with what were investigated so far. Predicted gamma-ray emission profiles and spectra differ depending on models of cluster formation as well as particle acceleration, and thus, by detecting or constraining them, one could learn important physics thereof, which is still completely missing and well awaited.

In this paper, we take a deeper look at the *Fermi*-LAT data for GeV gamma-ray emission from the Coma cluster and its possible diffuse emission induced by CR interactions. We chose Coma because it is one of the best studied clusters, which is located in a local volume (its distance is about 100 Mpc). It also shows evidence of recent dynamical activities such as particle accelerations, as seen from presence of a giant radio halo and a radio relic. Together with the fact that there are no AGN found in the LAT data, these make Coma an ideal environment to test CR-induced gamma-ray emission. We perform dedicated analyses of 63-month *Fermi*-LAT data using well-motivated models for spatial emission distribution. Besides the simplest point-source model, we investigate (1) models based on hydrodynamical simulations of the cluster formation that also trace interactions of CR protons with the ICM; (2) a model motivated by spatial profile of the radio relic, and (3) disk and ring-like profiles motivated by scenarios where primary electrons accelerated by accretion shocks dominates the cluster high-energy emission. We find no positive signatures in any of these scenarios, and thus, put the most constraining upper limits to date on the gamma-ray flux from Coma for each model and interpret them in terms of constraints on parameters of cluster formation and CR physics.

This paper is organized as follows. In Section 2, we describe details of the *Fermi*-LAT data analyses for Coma. Several theoretical model templates of the gamma-ray emission are explained in Section 3. We present our results in Section 4 and conclude in Section 5.

2 DATA ANALYSIS

We analysed 63 months (2008-08-04 15:43:37 to 2013-11-08 03:01:59) of *Fermi*-LAT *reprocessed* Pass 7 (P7REP) data of the Coma galaxy cluster using *Fermi Science Tools* (v9r32p5).² We adopted the standard event selection cuts suggested by the LAT collaboration and analyzed events between 100 MeV and 100 GeV. We analyzed both SOURCE and CLEAN events (*Fermi* event class 2 and 3, respectively), adopting the corresponding latest instrumental response functions (P7REP_V15), and we found good agreement between the two. In the following, we report the results for the standard *binned* likelihood analysis of the SOURCE events only.

We select a region of interest (ROI) of 10° of radius around the Coma cluster center (RA = $194^\circ 95$, DEC = $27^\circ 94$). We then bin the data into 0.1 pixels and 30 logarithmic steps in energy. This angular size is chosen to match the size of the point spread function achieved by *Fermi*-LAT at the highest energies, while it is significantly worse at low energies (about 10° and 1° at 100 MeV and 1 GeV, respectively; Fermi-LAT Collaboration 2012). The left panel of Figure 1 shows the photon count map of $14^\circ \times 14^\circ$, used for our binned analysis. The corresponding exposure map is computed for an area of $40^\circ \times 40^\circ$ centered on the cluster.

As a first step, we performed the analysis including all 26 point sources within 15° from the cluster center, found in the 2-year *Fermi* catalog (2FGL; Nolan et al. 2012) plus the latest templates for the Galactic and extragalactic backgrounds provided by the LAT collaboration (*gll_iem_v05* and *iso_isource_iv05*, respectively). The point sources are modeled with the spectral characteristics given in the 2FGL. We allowed the spectral parameters of the 22 sources within the ROI to vary in the likelihood analysis as well as the normalization of the diffuse background components. Note that no point sources are found within 3° from the cluster center in the 2FGL. The parameters of the other sources are kept fixed to the 2FGL values.

This model turns out to describe nicely the selected data, without the need of adding any more point sources or diffuse components. In Figure 1, we show an image of the best-fit model (center) as well as the residual map (right). The latter is obtained by subtracting the model from the photon count map in the left panel of Figure 1, and then by dividing again by the model. It is a residual map in units of percent and fluctuates between -1% and 2% , and as shown below, is consistent with random fluctuations.

The cluster models that we test feature diffuse gamma-ray emission on a very large scale and with quite low surface brightness. Such kind of emission could be buried in the background emission, and hence, a proper analysis is

¹ <http://fermi.gsfc.nasa.gov/>

² <http://fermi.gsfc.nasa.gov/ssc/data/analysis/>

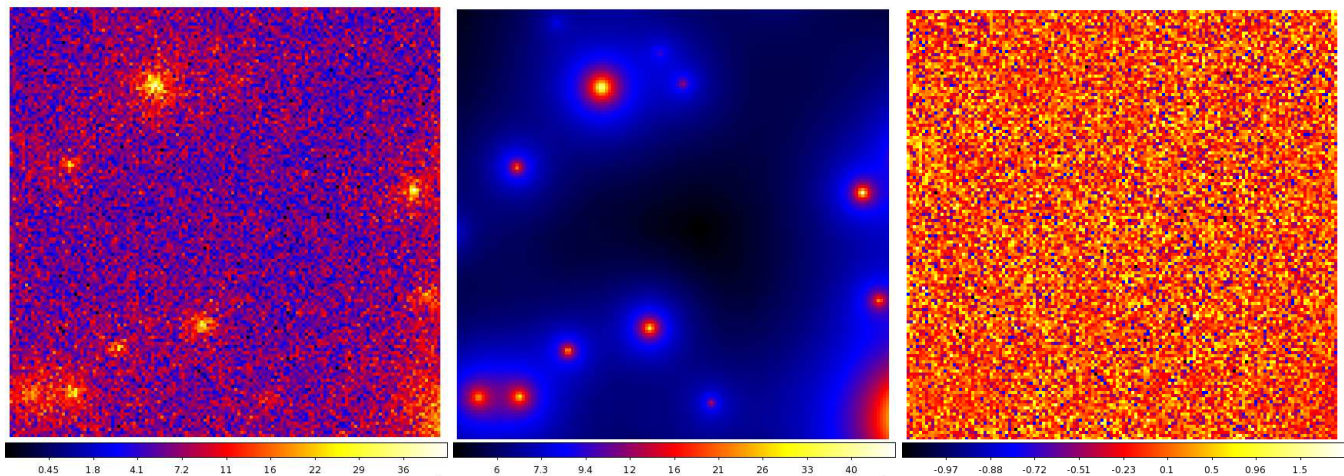


Figure 1. *Left.* LAT photon count map for an area of $14^\circ \times 14^\circ$ around the Coma galaxy cluster (whose center lies at the center of the image) obtained from about 5 years of observations. The cluster virial radius is about 1.3° . *Center.* Model count map for the basic analysis of the data with the 2FGL point sources, Galactic and extragalactic backgrounds. *Right.* Residual map in percents obtained as $(\text{counts} - \text{model})/\text{model}$. All maps are in square-root scale for visualization purposes.

needed in order to draw conclusions. Therefore, we run separate likelihood analysis with models including the point-sources, Galactic and extragalactic backgrounds, in addition to a given diffuse template for the cluster emission. Those are described in detail in the next section.

Before to proceed with the diffuse templates, as a second step, we placed an additional point-source (PS), modeled with a power-law E^Γ , at the Coma center. We performed again the binned likelihood analysis with a fixed spectral index $\Gamma = -2$. We find that the test statistics (TS ; Neyman & Pearson 1928) significance for this central point source is 0.³ We summarize the fit results, together with the obtained upper limits (ULs), in Table 1.

In order to compare with the latest constraints obtained from Fermi-LAT Collaboration (2013), we calculate the UL for their extended model (which corresponds to our PP model; see next section) for energies above 500 MeV obtaining $3.2 \times 10^{-10} \text{ cm}^{-2} \text{ s}^{-1}$. Fermi-LAT Collaboration (2013) obtained $4 \times 10^{-10} \text{ cm}^{-2} \text{ s}^{-1}$. Note that we adopt slightly different radius, mass and gas density values for the cluster modeling with respect to Fermi-LAT Collaboration (2013) which imply that our total flux above 500 MeV is a factor of about 1.1 larger. We achieve a more stringent UL due to this choice and thanks to the longer observation time (they used 48 months of data). Note also that while Fermi-LAT Collaboration (2013) uses CLEAN events, we report the result for the SOURCE events.

3 DIFFUSE EMISSION FROM COSMIC RAYS

In this section, we describe in detail the tested diffuse emission models. We show some relevant model templates used in our analysis in Fig. 2.

³ Note that in the background-only case, the TS value can be converted to the usual definition of significance as $\sqrt{TS}\sigma$ (e.g., Fermi-LAT Collaboration 2013).

3.1 Gamma Rays from Pion Decays

Pinzke & Pfrommer (2010), hereafter PP, performed hydrodynamical simulations of galaxy clusters considering, in particular, diffusive shock acceleration at structure formation shocks. They provided predictions for the gamma-ray emission from CR protons and electrons, and showed that the emission coming from pion decays dominates over the IC emission of both primary and secondary electrons for gamma-rays with an energy above 100 MeV. They then provide a semi-analytical model for the pion-decay-induced emission that depends on a given cluster mass and ICM density. The integral gamma-ray flux above the energy E can be expressed as follows:

$$F_{\gamma, \text{PP}}(> E) = A_p \lambda_{\gamma, \text{PP}}(> E) \int_V k_{\text{PP}}(R) dV, \quad (1)$$

where $\lambda_{\gamma, \text{PP}}(> E)$ and $k_{\text{PP}}(R)$ contain the spectral and spatial information, respectively, and are given in PP. A_p is a dimensionless scale parameter related to the maximum CR *proton* acceleration efficiency ξ_p for diffusive shock acceleration, which is the maximum ratio of CR energy density that can be injected with respect to the total dissipated energy at the shock.⁴ $A_p = 1$ for $\xi_p = 0.5$, and decreases for smaller efficiencies obeying a non-linear relation (PP). However, note

⁴ The CR proton acceleration efficiency attains its maximum, ξ_p , for high Mach number shocks, while it is lower for lower Mach numbers. The exact Mach number dependence of the acceleration efficiency is very uncertain. In this work we use as reference the Pinzke & Pfrommer (2010) simulations that depend on the Enßlin et al. (2007) model for diffusive shock acceleration for which ξ_p , in the case of interest for clusters, is reached for Mach numbers of about 3. We note, however, that more detailed models such as the Kang & Ryu (2013) model, in the context of *non-linear* diffusive shock acceleration, shows a different dependence, and the acceleration efficiency saturates at higher Mach numbers with respect to Enßlin et al. (2007). Because of the early saturation in the Enßlin et al. (2007) model, our constraints on the efficiency could be regarded as conservative in the low Mach number regime where more refined models show lower efficiencies.

that the relation A_p – ξ_p is linear for CR protons with an energy $\gtrsim 10$ GeV which corresponds to pion decay emission with energies $\gtrsim 1$ GeV (A. Pinzke, private communication).

The PP predictions have already being challenged by recent gamma-ray observations (MAGIC Collaboration 2010, 2012; Pinzke et al. 2011; Han et al. 2012; VERITAS Collaboration 2012; Fermi-LAT Collaboration 2013), suggesting either that the maximum CR proton acceleration efficiently at shocks is significantly lower than 50%, an optimistic value adopted in simulations, or the presence of CR streaming and diffusion out of the cluster core (Enßlin et al. 2011; Wiener et al. 2013; Zandanel et al. 2014b).

We test the PP spatial and spectral semi-analytical model for the Coma cluster, where the cluster mass is taken from Reiprich & Böhringer (2002) and the ICM radial profile from Briel et al. (1992). In the PP model, only about 5% of the total emission is coming from radii beyond the virial radius, and therefore we decide to limit our analysis within the virial radius⁵ $R_{200} = 2.3 (h/0.7)^{-1}$ Mpc.

Note, however, that assuming the magnetic field in the cluster is distributed according to

$$B(r) = B_0 \left(\frac{\rho_{\text{gas}}(r)}{\rho_{\text{gas}}(0)} \right)^{\alpha_B}, \quad (2)$$

where ρ_{gas} is the ICM distribution, $B_0 = 5 \mu\text{G}$ and $\alpha_B = 0.5$ as suggested by Faraday rotation (FR) measurements in Coma (Bonafede et al. 2010), the radio synchrotron emission (see, e.g., appendices of Zandanel et al. 2014b) predicted by the PP semi-analytical model does not match the spatial profile of the giant radio halo of the cluster at 1.4 GHz (Deiss et al. 1997), being much more peaked, as shown in Figure 3. Additionally, it overproduces the central radio emission for a maximum acceleration efficiency $\gtrsim 5\%$ (assuming a linear scaling of A_p with ξ_p).

Zandanel et al. (2014b), hereafter ZPP, extended the PP semi-analytic model with the inclusion of an effective parameterization for CR transport phenomena, effectively redefining $k_{\text{PP}}(R)$ of eq. (1). Since the CR transport is determined by competition among advection due to turbulent motion of gas, CR streaming, and diffusion, its efficiency can be represented by a parameter,

$$\gamma_{tu} = \frac{\tau_{st}}{\tau_{tu}}, \quad (3)$$

i.e., a ratio of a characteristic time scale of streaming, τ_{st} , and that of turbulence, τ_{tu} (Enßlin et al. 2011). The parameter γ_{tu} ranges from 100, for highly turbulent cluster and centrally peaked CR distributions, to 1, for relaxed clusters and flat distributions as CRs move toward the outskirts. When $\gamma_{tu} \geq 100$, the model reproduce the advection-dominated case of Pinzke & Pfrommer (2010), where CR transport treatment is not included. We test the ZPP model for the case of $\gamma_{tu} = 2$ (ZPP-2), matching the observed surface brightness profile of the Coma radio halo at 1.4 GHz (see Figure 3). Note that Coma is classified as merging cluster and one would expect it to be turbulent and not relaxed. Therefore, according to Enßlin et al. (2011), high γ_{tu} values and a centrally peaked CR distribution should be realized.

⁵ Defined with respect to a density that is 200 times the critical density of the Universe.

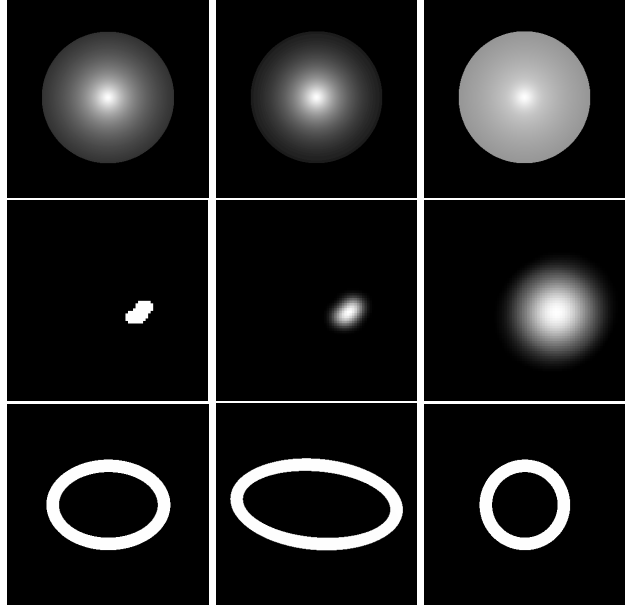


Figure 2. Some of the diffuse emission templates models used in the analysis. Top row shows, from left to right, $4^\circ \times 4^\circ$ images of the PP, ZPP-100 and ZPP-2 models, in logarithmic scale. The middle row show the $8^\circ \times 8^\circ$ image of the relic template, where the central and right images are after being convolved with a Gaussian of width of 1° and 4° , respectively, to give an idea of the effect of the *Fermi*-LAT point-spread function at different energies. The bottom row shows, from left to right, $8^\circ \times 8^\circ$ images of the ellipse, tilted ellipse and ring models.

Wiener et al. (2013) found a solution to this problem showing that, when considering turbulent damping, turbulence may promote outward streaming more than inward advection, therefor allowing for flat CR profiles also in turbulent clusters.

At this point one may ask how representative is the giant radio halo of the Coma cluster, particularly the parameters' values needed for its modeling. While we cannot say with certainty that these are common to all merging clusters hosting diffuse radio emission without an extensive analysis of the whole sample, we note that ZPP found the same characteristics, in particular the need for low γ_{tu} values, in the giant radio halo of the merging cluster Abell 2163. This is due to the large radial extension and shallow profile of the surface brightness of these objects, which appear to be a common property among giant radio halos (Feretti et al. 2012).

However, ZPP showed that even in the extreme case of a flat CR distribution, $\gamma_{tu} = 1$, it is not possible to hadronically reproduce the 352 MHz surface brightness of the giant radio halo of Coma (Brown & Rudnick 2011). This favors re-acceleration models (Brunetti et al. 2012), or hybrid scenarios where only part of the radio emission is of hadronic origin (see ZPP for an extensive discussion). In this case, a centrally peaked CR distribution could still be realized and only partially contribute to the total observed radio emission. We therefore test also a ZPP model with $\gamma_{tu} = 100$ (ZPP-100). Note that this is decreasing slightly faster toward the cluster outskirts than the PP model because of

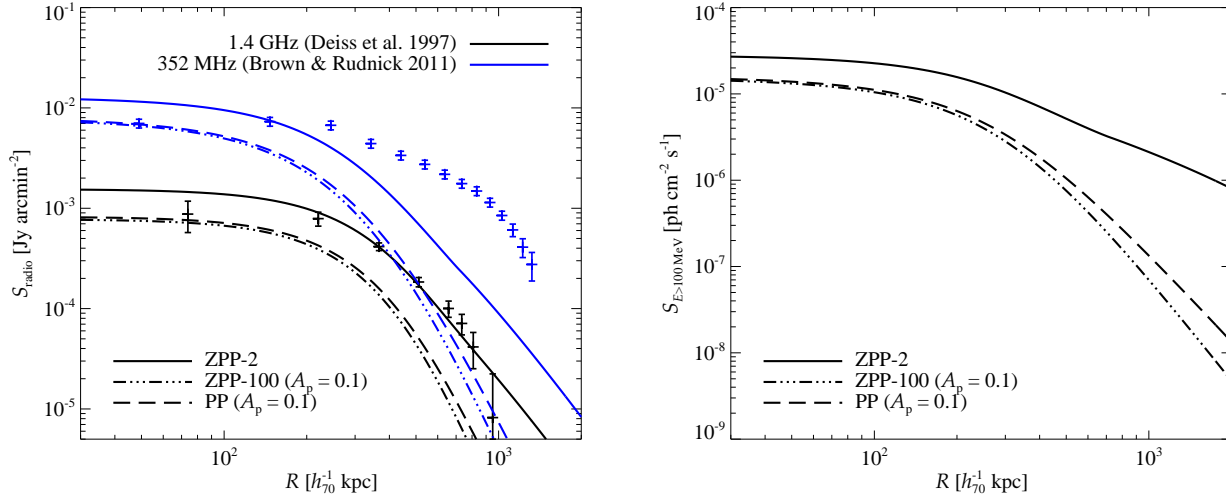


Figure 3. Surface brightness of the Coma cluster calculated as in ZPP. *Left.* Surface brightness of the giant radio halo at 352 MHz (Brown & Rudnick 2011) and 1.4 GHz (Deiss et al. 1997). Shown are the ZPP-2 model, and the ZPP-100 and PP models scaled down with $A_p = 0.1$ such that they do not overshoot the radio emission. *Right.* Gamma-ray surface brightness for energies above 100 MeV for the ZPP-2 model, and ZPP-100 and PP models scaled down with $A_p = 0.1$.

the inclusion of the characteristic radial decline of the temperature (ZPP; see Figure 2 and 3).

Also for the ZPP models we limit our analysis within R_{200} . Both for PP and ZPP models, we let the normalization of the emission to vary. The spectral shape is fixed to the PP model prediction, featuring the characteristic pion bump at GeV energies followed by a concave spectrum that approaches a power-law with spectral index of about 2.2 at TeV energies (see Figure 12 of PP). We warn that by fixing the CR spectra to the PP findings, we exclude a potential free parameter that would affect our conclusions (see, e.g., MAGIC Collaboration 2012; VERITAS Collaboration 2012).

3.2 Gamma Rays from Inverse-Compton Scattering

Kushnir & Waxman (2009) developed an analytical model, adopting a CR power-law energy spectrum with a spectral index of -2 , and predicted that the IC emission from primary electrons accelerated at accretion shocks dominates over the pion-decay induced emission. Considering the differences in acceleration efficiency and injected spectra may reconcile the findings by Kushnir & Waxman (2009) and PP (see Fermi-LAT Collaboration 2013, for a detailed discussion). However, instead of the centrally concentrated gamma-ray emission from neutral pion decays, Kushnir & Waxman (2009) found a spatially extended IC-induced emission out to the accretion shocks beyond the cluster's virial radius. This model predicts a practically flat gamma-ray emission up to the outer accretion shocks location where it should then peak (see Fig. 2 of Kushnir & Waxman 2009). We therefore test this model with a flat disk template of 1° of radius. We consider a power-law spectrum with a fixed $\Gamma = -2$.

Kushnir & Waxman (2009) predict that the radio emission should be dominated by secondaries. The correspond-

ing profile of the radio surface brightness is similar to the ZPP model with a low γ_{tu} value, potentially being able to explain the 1.4 GHz data for the Coma giant halo but also suffering the same problems discussed in the previous section when trying to reproduce the 352 MHz data. Additionally, we note that Kushnir & Waxman (2009) assume a constant magnetic field in the cluster core, which is in contrast with FR estimates in Coma (Bonafede et al. 2010), and implies a shallower radio profile.

Accretion of intracluster gas should generate strong virial shock waves around galaxy clusters and, according to several scenarios, this could potentially lead to ring-like emission features at different frequencies (Loeb & Waxman 2000; Totani & Kitayama 2000; Waxman & Loeb 2000; Miniati 2002; Keshet et al. 2003, 2004; Kocsis et al. 2005; Kushnir & Waxman 2010). Note however that latest state-of-the-art cosmological hydrodynamical simulations of galaxy clusters do not show the presence of such features (Pfrommer et al. 2008; Pfrommer 2008; Pinzke & Pfrommer 2010).

Recently, Keshet et al. (2012) claimed the detection of a ring-like structure in the gamma-ray sky map of the Coma cluster in the VERITAS data (VERITAS Collaboration 2012) and interpreted this as IC-induced emission due to accretion shocks around the cluster. Therefore, we searched for the presence of this structure: it is a 0.5° -wide elliptical shape with a semi-minor axis of about 1.3° , elongated toward the east-west direction. We consider cases where the semi-major axis is of 2° , and of 3° with the structure tilted towards the southwest direction for 5° . The latter case corresponds to the best fit of Keshet et al. (2012), confirmed also by comparison with simulations by Keshet et al. (2003). We refer to these as ellipse models. We additionally consider the case of a 0.5° -wide ring with radius of R_{200} (ring model). In all the cases, we uniformly fill the tested structure, and we consider a power-law spectrum with a fixed $\Gamma = -2$.

We finally consider also a phenomenological tem-

plate based on the radio relic observed in Coma outskirts, which is associated with structure-formation phenomena. Recent observations, both in radio and X-rays, support the idea that it is connected to an infall shock front due to the NGC 4839 group falling onto the cluster (Brown & Rudnick 2011; Ogrea & Brüggen 2013; Akamatsu et al. 2013; Simionescu et al. 2013) rather than a cluster-merger shock. Either way, the corresponding CR electrons could generate IC gamma-ray emission. We use the Green Bank Telescope (GBT) observation at 1.4 GHz presented by Brown & Rudnick (2011) to generate a spatial template for the relic. We can use such an approach if we assume that the magnetic field is almost uniform across the relic (Bonafede et al. 2013). This approximation is well justified in our case considering the poor *Fermi* angular resolution with respect to radio observations. We therefore use the outermost contour of the GBT radio relic image from Figure 2 of Brown & Rudnick (2011) to construct its spatial template, which we uniformly fill. We refer to this as the relic model. We let the normalization to vary, and we use a power-law for the radio spectrum with a fixed $\Gamma = -1.18$, as inferred from the observed radio spectrum (Thierbach et al. 2003).

4 RESULTS AND IMPLICATIONS

In the following subsections we discuss the implications of our findings for each of the considered models. Table 1 summarizes the obtained ULs.

4.1 Pion Decay Emission

In the PP and ZPP-100 models, assuming a maximum CR proton acceleration efficiency of 50%, we would expect a total flux above 100 MeV and within R_{200} of 4.14 and $3.24 \times 10^{-9} \text{ cm}^{-2} \text{ s}^{-1}$, respectively. The obtained ULs (see Table 1) are a factor of 0.26 and 0.28 of the theoretical expectations, respectively. This suggest that the maximum CR proton acceleration efficiency at shocks must be lower than about 15%, or implies the presence of significant CR propagation out of the cluster core in order to lower the central emission. Our ULs also set a limit to the CR-to-thermal pressure in the Coma cluster, $X_{\text{CR}} = P_{\text{CR}}/P_{\text{th}}$ (volume-averaged within R_{200} ; see, e.g., ZPP), to be less than approximately 1.3% and 0.6% for the PP and ZPP-100 model, respectively, within R_{200} . Note that the limits on both the flux and CR pressure for the PP model are more stringent than those obtained in the previous work on the Coma cluster (Pinzke et al. 2011; Han et al. 2012; VERITAS Collaboration 2012; Fermi-LAT Collaboration 2013).

If CR streaming and diffusion are in action in the cluster, we would expect a much flatter emission profile which is represented by the ZPP-2 model. This model matches the 1.4 GHz Deiss et al. (1997) surface brightness profile of the Coma radio halo, assuming the magnetic field is distributed accordingly to FR measurements ($B_0 = 5 \mu\text{G}$, $\alpha_B = 0.5$; Bonafede et al. 2010). The predicted gamma-ray flux above 100 MeV within R_{200} is $2.36 \times 10^{-9} \text{ cm}^{-2} \text{ s}^{-1}$. In this case, X_{CR} within R_{200} is much higher, about 17%, as streaming causes the CR pressure to rise in the cluster's outskirts with

Table 1. Results of the binned likelihood analyses for 63 months of the *Fermi*-LAT data of the Coma cluster. The analyses include all 26 point sources within 15° from the cluster center, the extragalactic and galactic backgrounds, and a given model. All spectral templates are modeled as power law in the form of $dN/dE = N_0 E^\Gamma$, except for PP and ZPP where the spectrum provided by the corresponding models is used. For each fit, reported are the resulting TS significance, spectral index Γ and flux UL F_{UL} integrated over 100 MeV–100 GeV with 95% confidence level.

model	notes	TS	Γ	F_{UL} [$\times 10^{-9} \text{ cm}^{-2} \text{ s}^{-1}$]
PS		0.0	−2	0.62
PP		0.3	−	1.08
ZPP-100	$\gamma_{tu} = 100$	0.1	−	0.92
ZPP-2	$\gamma_{tu} = 2$	1.3	−	1.81
Relic		0.0	−1.18*	0.09
Ellipse		0.0	−2	2.49
Ellipse	tilted	0.0	−2	1.74
Ring		0.2	−2	2.59
Disk		1.5	−2	2.91

Notes. *The spectral index of the relic template is assumed to be as inferred from the observed radio spectrum (Thierbach et al. 2003).

respect to the ICM pressure (see Figure 2 of ZPP). However, X_{CR} reduces to 2.7% within $R_{200}/2$. The corresponding flux UL shown in Table 1, $1.81 \times 10^{-9} \text{ cm}^{-2} \text{ s}^{-1}$, challenges the ZPP-2 model. However, a slightly different choice of parameters can still circumvent this limit while reproducing the 1.4 GHz radio data (ZPP), e.g., in case of $\gamma_{tu} = 3$ and $\alpha_B = 0.4$, the predicted gamma-ray flux above 100 MeV is about $1.3 \times 10^{-9} \text{ cm}^{-2} \text{ s}^{-1}$, whereas the UL hardly changes.

As explained above, an intriguing alternative is that of an hybrid scenario where the hadronic component would make up only the central part of the observed radio emission (ZPP). If this would be the case, the more centrally peaked PP and ZPP-100 models would still be a viable option, but requiring that they do not over-shoot the radio emission both at 1.4 GHz and at 352 MHz. Assuming $B_0 = 5 \mu\text{G}$ and $\alpha_B = 0.5$ sets both the PP and ZPP-100 fluxes to be a factor of about 0.1 of the theoretical expectations presented at the beginning of this section, corresponding to a maximum CR proton acceleration efficiency of about 5%. These are a factor of three lower than the *Fermi*-LAT ULs presented here. However, there is a wide parameter space between a flat profile ($\gamma_{tu} \sim 1$) and a totally advection-dominated profile ($\gamma_{tu} \sim 100$), leaving room for a possible detection of pion-decay emission in clusters with *Fermi*-LAT or Cherenkov telescopes, in particular with the planned Cherenkov Telescope Array (CTA).⁶ Indeed, if such an hybrid scenario were realized in nature, the synergy of radio and gamma-ray observations would be very important in understanding the relevance of CR protons in clusters, and also in breaking the degeneracy with magnetic field estimates and radio modeling.

⁶ <http://www.cta-observatory.org/>

Another alternative is that the observed radio emission is not of hadronic origin at all, but it is generated by re-acceleration of a seed population of electrons. This seed population could be made of secondary electrons, from CR proton-proton interactions with the ICM, that are re-accelerated to emitting energies at a later stage (Brunetti et al. 2012). Also in this case, a corresponding pion-decay induced emission is expected, but at a much lower level. Using the spectra shown in Figure 6 of Brunetti et al. (2012), we estimated that the integral gamma-ray flux for energies 100 MeV–100 GeV would be at a level of $2.6\text{--}1.4 \times 10^{-10} \text{ cm}^{-2} \text{ s}^{-1}$ in this scenario, almost one order of magnitude lower than our current ULs.

4.2 Inverse-Compton Emission

In this section we discuss the implications of our analysis for the IC-induced emission from accretion shocks, and connected to the radio relic of Coma.

4.2.1 Accretion Shocks

Kushnir & Waxman (2009) predicted a IC-induced flux above 100 MeV and within 1° from the center of the Coma cluster of about $10^{-8} \text{ cm}^{-2} \text{ s}^{-1}$. Our UL obtained with the disk template is $2.9 \times 10^{-9} \text{ cm}^{-2} \text{ s}^{-1}$, about a factor of 3 below their prediction. This limits the CR *electron* acceleration efficiency at shocks to be $\xi_e < 1\%$. The same is true for the prediction of Keshet et al. (2003). The absence of any kind of ring-shaped emission around the Coma cluster, and the comparison of our integral flux ULs above 100 MeV of about $2.5 \times 10^{-9} \text{ cm}^{-2} \text{ s}^{-1}$ with the predicted flux of about $4 \times 10^{-8} \text{ cm}^{-2} \text{ s}^{-1}$ (see eq. (11) of Keshet et al. 2012), implies that the CR electron efficiency at shocks is $\xi_e < 0.5\%$. This is consistent with *Fermi* not having detected any of these structures (Keshet et al. 2003).

4.2.2 The Radio Relic

We model the emission of the radio relic of Coma using the data compiled by Thierbach et al. (2003). As explained above, the electrons generating the radio emission can also emit hard X-rays and gamma-rays via IC scattering off the CMB photons. We therefore compute their synchrotron and IC emission (Blumenthal & Gould 1970; Rybicki & Lightman 1979), as done in Murgia et al. (2010). We do not make any a priori assumption on the electron acceleration mechanism, but simply adopt a phenomenological approach. We assume a power-law electron distribution $n(E) \propto E^{-\alpha_e}$. The free parameters are the normalization of the electron distribution, spectral index α_e , integration limits (E_{\min}, E_{\max}), and the volume averaged magnetic field B_V across the relic region. The electron spectral index is well determined by the slope of radio spectrum $\alpha_\nu = 1.18$ (Thierbach et al. 2003) and fixed at $\alpha_e = 2\alpha_\nu + 1 = 3.36$. The low- and high-energy cutoffs of the electron distribution are not constrained by current data; in fact, the existing radio measurements allow us only to establish $E_{\min}/m_e c^2 \lesssim 2500$ and $E_{\max}/m_e c^2 \gtrsim 2 \times 10^5$. The low-energy cutoff is typically determined by the Coulomb losses and we fix it

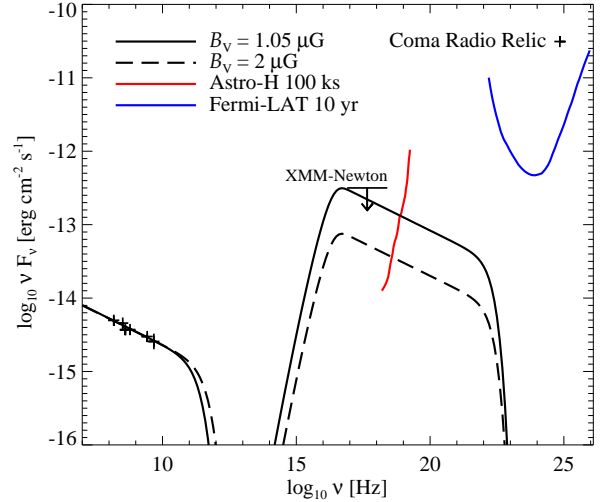


Figure 4. Spectral energy distribution of the radio relic of the Coma cluster. The radio data is taken from the Thierbach et al. (2003) compilation, while the *XMM-Newton* UL is from Feretti & Neumann (2006). We show the synchrotron and IC emission for $B_V = 1.05$ and $2 \mu\text{G}$. Also shown are the point-source sensitivities expected for Astro-H HXI in 100 ks Takahashi et al. (2012) and for *Fermi*-LAT in 10 yr (Funk & Hinton 2013).

at $E_{\min}/m_e c^2 = 200$ (see, e.g., Sarazin 1999). For the high-energy cutoff we assume $E_{\max}/m_e c^2 = 2 \times 10^5$, corresponding to electron energies of 100 GeV. By varying the normalization such that the IC emission do not exceed the high-energy ULs, we can estimate a lower limit for the magnetic field needed to generate the observed synchrotron radio emission. We found this to be constrained by the X-ray UL from *XMM-Newton* observations (Feretti & Neumann 2006) as $B_V \gtrsim 1 \mu\text{G}$. We show this in Figure 4. These values are consistent with the estimate of $B_V = 2 \mu\text{G}$ obtained from FR measurements in the cluster outskirts by Bonafede et al. (2013). This is about a factor of 6 higher than what previously obtained by extrapolating eq. (2) to the relic location (Bonafede et al. 2010) and implies magnetic amplification in the relic region (Bonafede et al. 2013). In Figure 4, we also show the case where we fix the magnetic field to $B_V = 2 \mu\text{G}$.

Not surprisingly, the X-ray upper limit obtained with *XMM-Newton* (Feretti & Neumann 2006) is much more constraining than *Fermi*-LAT. In fact, the *Fermi*-LAT extragalactic (point-source) sensitivity for 10 years of observation (Funk & Hinton 2013) is well above the expected IC flux. Therefore, the high-energy emission associated with the electron population generating the Coma radio relic seems out of reach of existing and future-planned gamma-ray instruments. In this case, a much more exciting picture is that of the current and next generations of X-ray satellites, such as NuSTAR (launched in June 2012; Harrison et al. 2013) and Astro-H (to be launched in 2014; Takahashi et al. 2012). Indeed, the Astro-H Hard X-ray Imager (HXI) sensitivity curve (for a 100 ks exposure) shown in Figure 4 demonstrates potential to finally break the radio–X-ray degeneracy in determining the magnetic field value. We warn, however, that

the radio relic emission region⁷ is about 0.1 deg^2 , while the reported HXI sensitivity curve is for a point source and the HXI angular resolution is below 2 arcmin (Takahashi et al. 2012).

Note that the pion-decay emission should be suppressed at the relic due to the lack of enough target ICM protons for hadronic interactions. Recently, Vazza & Brüggen (2014) tested the acceleration of protons by shock waves propagating through clusters against *Fermi*-LAT ULs, finding, similarly to this work, that the resulting central hadronic-induced emission lies very close to them. Their prediction for the hadronic-induced gamma-ray emission at the Coma relic, in the energy range of 200 MeV to 100 GeV, goes from 0.4 to $3 \times 10^{-12} \text{ cm}^{-2} \text{ s}^{-1}$ depending on the adopted model (F. Vazza, private communication).⁸ This is very low, as expected from the low density of target protons at the relic location (Simionescu et al. 2013). Our UL on the relic template in this energy range is around $0.7 \times 10^{-10} \text{ cm}^{-2} \text{ s}^{-1}$, about two orders of magnitude above expectations. Note also that this UL is significantly more stringent than the others we obtained because of the steeper spectrum.

We refrain from performing a similar synchrotron plus IC phenomenological modeling of the central giant radio halo of Coma as the corresponding volume average magnetic field, of about $2 \mu\text{G}$ (Bonafede et al. 2010), together with the extension of the radio emission area, of about 1 deg^2 , suggest that it would be extremely difficult to aim for a detection of the corresponding IC-induced emission, even with the next-generation X-ray satellites (see also Wik et al. 2011).

4.3 Diffuse Extragalactic Gamma-ray Background

The constraints derived here not only affect particle acceleration modeling in clusters of galaxies, but also the possible contribution to the extragalactic gamma-ray background (e.g., *Fermi*-LAT Collaboration 2010c).

Loeb & Waxman (2000) estimated that the possible IC-induced emission at accretion shocks could be high enough to entirely explain the gamma-ray background. Keshet et al. (2003), by using *N*-body simulations, estimated this to be about 10% for $\xi_e = 5\%$ (see also Gabici & Blasi 2003). Our ULs imply that the possible IC-induced contribution must be lower than 1%.

One can ask how much of the possible pion-decay-induced emission in galaxy clusters could contribute to the extragalactic gamma-ray background. Ando & Nagai (2008), with a simple analytical model, estimated this to

be less than a few percents (see also Colafrancesco & Blasi 1998). By making use of the mock galaxy clusters catalogs of Zandanel et al. (2014a),⁹ which include the prediction for the pion-decay induced emission in galaxy clusters following the ZPP prescription, we estimate this to be less than 1%.

Summarizing, this means that acceleration of CR protons and electrons in galaxy clusters gives a negligible contribution to the diffuse extragalactic gamma-ray background. We note, however, that if the other possible contributions, such as from blazars and star-forming regions, are well understood, this could be a potentially interesting way to study relativistic particles in galaxy clusters.

5 CONCLUSIONS

Since generation of shocks and particle acceleration in the shocks are generic predictions of large-scale-structure formation scenarios, one expects gamma-ray emission from clusters of galaxies by secondaries from CR proton-proton interactions with the ICM, and by IC scattering of CR electrons off the CMB. In this paper, we analyzed 63-month (P7REP) data from *Fermi*-LAT photons between 100 MeV and 100 GeV from the Coma cluster, one of the best studied nearby galaxy clusters. Coma also shows recent activity of a merger and accretion, and has both a radio relic and giant radio halo. These observations make Coma a promising gamma-ray source, such that one is able to test CR energy content in the galaxy cluster and also particle acceleration mechanisms. We tested several template models of the gamma-ray emission from Coma and found no positive signature corresponding to any of these models. We, however, obtained the most stringent constraints to date on the Coma cluster above 100 MeV, as summarized below (see also Table 1).

(1) *Point-source model.* We obtained a point-source flux upper limit, assuming a power-law energy spectrum with an index of -2 , of $F_{\text{UL}} = 0.6 \times 10^{-9} \text{ cm}^{-2} \text{ s}^{-1}$, which is better by a factor of a few compared with previous studies (e.g., Ando & Nagai 2012). Note, however, that a softer spectrum would cause the UL to increase (as in *Fermi*-LAT Collaboration 2013).

(2) *Pion decays.* In this case, the spatial profile depends on the efficiency of CR turbulent motion compared with that of streaming. We chose several profiles and found that the flux limits are $F_{\text{UL}} \simeq (0.9\text{--}1.8) \times 10^{-9} \text{ cm}^{-2} \text{ s}^{-1}$, where the latter (former) value is for a more (less) extended model as a result of higher (lower) efficiency of streaming. These limits constrain the predictions of Pinzke & Pfrommer (2010) and Zandanel et al. (2014b), which implies either that maximum CR proton acceleration efficiencies at shocks are lower than about 15%, or the presence of significant CR propagation out of the cluster core. We also note that by comparing the advection-dominated centrally peaked profiles to the observed radio emission, the maximum CR proton acceleration efficiency is limited to be below about 5%. Note, however, that these conclusions rely on the assumption of mag-

⁷ The emission modeled in Figure 4 corresponds to the radio relic region reported by Thierbach et al. (2003), which is about $800 \times 400 \text{ kpc}$, corresponding to about 400 arcmin^2 . Note that the total relic extension reported by Brown & Rudnick (2011), on which we base our relic template for the analysis of Section 2, is significantly larger with a transverse extent of about 2 Mpc. However, due to the very steep spectrum of the radio relic, we do not expect this to change our conclusion for the gamma-ray detectability.

⁸ Note that Vazza & Brüggen (2014) assume that relics trace outward propagating shocks, and this is uncertain in the case of the Coma cluster as the relic may be tracing an infall shock (Brown & Rudnick 2011; Ogresh & Brüggen 2013; Akamatsu et al. 2013; Simionescu et al. 2013).

⁹ The Zandanel et al. (2014a) mock catalogs have been taken from the MultiDark online database (www.multidark.org, Riebe et al. 2013).

netic field estimates from FR measurements (Bonafede et al. 2010) and on a fixed CR spectrum (PP).

(3) *Inverse-Compton Emission.* Motivated by predictions for IC-induced emission from electrons accelerated at accretion shocks, we investigated both a disk and ring-like emission template. We found ULs of $F_{\text{UL}} = (1.7\text{--}2.9) \times 10^{-9} \text{ cm}^{-2} \text{ s}^{-1}$, which is not consistent with low-energy extrapolation of a recent claim of positive detection of such a ring-like feature in the VERITAS data (Keshet et al. 2012). Additionally, this limits the CR electron acceleration efficiency at shocks to be less than 1% both in the Keshet et al. (2003) and in the Kushnir & Waxman (2009) scenarios.

(3) *Radio Relic.* We adopted an emission profile consistent with the Coma radio relic, and looked for the corresponding gamma-ray emission. The radio emission from the relic is interpreted as a synchrotron radiation from non-thermal electrons, and there should be a corresponding high-frequency component due to IC scattering from the same electrons. The gamma-ray-flux upper limit is $F_{\text{UL}} = 0.9 \times 10^{-10} \text{ cm}^{-2} \text{ s}^{-1}$, but this is too weak to constrain the electron population. This is because the expected energy range of the IC scattering off CMB photons is in X-rays for an electron population matching the radio relic synchrotron emission. Instead, we find that the current (NuSTAR) and future (Astro-H) X-ray telescopes have excellent prospects for detecting this IC emission.

(4) *Diffuse Extragalactic Gamma-ray Background.* We conclude by noting that, following Keshet et al. (2003) our results imply that the possible IC-induced emission associated with structure formation shocks in clusters of galaxies can contribute to the diffuse extragalactic gamma-ray background by less than 1%. At the same time, using the Zandanel et al. (2014a) mock galaxy cluster catalogs, we estimate that also the possible pion-decay induced emission can contribute only by less than 1%. This renders the contribution to the diffuse extragalactic gamma-ray background due to the high-energy photons from structure-formation processes in clusters of galaxies negligible.

ACKNOWLEDGMENTS

We would like to thank Anders Pinzke and Christoph Weniger for useful discussions. We thank Franco Vazza for providing the pion-decay emission at the radio relic location as given by his model. FZ thank the support of the Spanish MICINN's Consolider-Ingenio 2010 Programme under grant MultiDark CSD2009-00064, AYA10-21231. The MultiDark Database used in this paper and the web application providing online access to it were constructed as part of the activities of the German Astrophysical Virtual Observatory as result of a collaboration between the Leibniz-Institute for Astrophysics Potsdam (AIP) and the Spanish MultiDark Consolider Project CSD2009-00064. The Bolshoi and MultiDark simulations were run on the NASA's Pleiades supercomputer at the NASA Ames Research Center. The MultiDark-Planck (MDPL) and the BigMD simulation suite have been performed in the Supermuc supercomputer at LRZ using time granted by PRACE. This work was supported by the Netherlands Organization for Scientific Research (NWO) through Vidi grant.

REFERENCES

- Akamatsu H., Inoue S., Sato T., Matsusita K., Ishisaki Y., Sarazin C. L., 2013, PASJ, 65, 89
- Ando S., Nagai D., 2008, MNRAS., 385, 2243
- Ando S., Nagai D., 2012, JCAP, 7, 17
- Blumenthal G. R., Gould R. J., 1970, Reviews of Modern Physics, 42, 237
- Bonafede A., Feretti L., Murgia M., Govoni F., Giovannini G., Dallacasa D., Dolag K., Taylor G. B., 2010, A&A, 513, A30+
- Bonafede A., Vazza F., Brüggén M., Murgia M., Govoni F., Feretti L., Giovannini G., Ogrean G., 2013, MNRAS
- Briel U. G., Henry J. P., Boehringer H., 1992, A&A, 259, L31
- Brown S., Rudnick L., 2011, MNRAS, 412, 2
- Brunetti G., Blasi P., Reimer O., Rudnick L., Bonafede A., Brown S., 2012, MNRAS, 426, 956
- Brunetti G., Lazarian A., 2007, MNRAS, 378, 245
- Brunetti G., Lazarian A., 2011, MNRAS, 410, 127
- Colafrancesco S., Blasi P., 1998, Astroparticle Physics, 9, 227
- Deiss B. M., Reich W., Lesch H., Wielebinski R., 1997, A&A, 321, 55
- Domainko W., Nedbal D., Hinton J. A., Martineau-Huynh O., 2009, International Journal of Modern Physics D, 18, 1627
- Enßlin T., Pfrommer C., Miniati F., Subramanian K., 2011, A&A, 527, A99+
- Enßlin T. A., Pfrommer C., Springel V., Jubelgas M., 2007, A&A, 473, 41
- Feretti L., Giovannini G., Govoni F., Murgia M., 2012, A&Ar, 20, 54
- Feretti L., Neumann D. M., 2006, A&A, 450, L21
- Fermi-LAT Collaboration, 2010a, JCAP, 5, 25
- Fermi-LAT Collaboration, 2010b, ApJ, 717, L71
- Fermi-LAT Collaboration, 2010c, Physical Review Letters, 104, 101101
- Fermi-LAT Collaboration, 2012, ApJS, 203, 4
- Fermi-LAT Collaboration, 2013, ArXiv:1308.5654
- Funk S., Hinton J. A., 2013, Astroparticle Physics, 43, 348
- Gabici S., Blasi P., 2003, Astroparticle Physics, 19, 679
- Galante N. et al., 2009, ArXiv:0907.5000
- Han J., Frenk C. S., Eke V. R., Gao L., White S. D. M., Boyarsky A., Malyshev D., Ruchayskiy O., 2012, MNRAS, 427, 1651
- Harrison F. A. et al., 2013, ApJ, 770, 103
- HESS Collaboration, 2009a, A&A, 502, 437
- HESS Collaboration, 2009b, A&A, 495, 27
- HESS Collaboration, 2012, A&A, 545, A103
- Huber B., Tchernin C., Eckert D., Farnier C., Manalaysay A., Straumann U., Walter R., 2013, A&A, 560, A64
- Kang H., Ryu D., 2013, ApJ, 764, 95
- Keshet U., Kushnir D., Loeb A., Waxman E., 2012, ArXiv:1210.1574
- Keshet U., Waxman E., Loeb A., 2004, ApJ, 617, 281
- Keshet U., Waxman E., Loeb A., Springel V., Hernquist L., 2003, ApJ, 585, 128
- Kiuchi R. et al., 2009, ApJ, 704, 240
- Kocsis B., Haiman Z., Frei Z., 2005, ApJ, 623, 632
- Kushnir D., Waxman E., 2009, JCAP, 8, 2
- Kushnir D., Waxman E., 2010, JCAP, 2, 25

- Loeb A., Waxman E., 2000, *Nature*, 405, 156
- MAGIC Collaboration, 2010, *ApJ*, 710, 634
- MAGIC Collaboration, 2012, *A&A*, 541, A99
- Miniati F., 2002, *MNRAS*, 337, 199
- Murgia M., Eckert D., Govoni F., Ferrari C., Pandey-Pommier M., Nevalainen J., Paltani S., 2010, *A&A*, 514, A76
- Neyman J., Pearson E. S., 1928, *Biometrika*, 20A, 175
- Nolan P. L. et al., 2012, *ApJS*, 199, 31
- Ogrean G. A., Brüggén M., 2013, *MNRAS*, 433, 1701
- Ogrean G. A., Brüggén M., van Weeren R. J., Röttgering H., Croston J. H., Hoeft M., 2013, *MNRAS*, 433, 812
- Perkins J. S., 2008, in *American Institute of Physics Conference Series*, Vol. 1085, American Institute of Physics Conference Series, Aharonian F. A., Hofmann W., Rieger F., eds., pp. 569–572
- Perkins J. S. et al., 2006, *ApJ*, 644, 148
- Pfrommer C., 2008, *MNRAS*, 385, 1242
- Pfrommer C., Enßlin T. A., 2004a, *A&A*, 413, 17
- Pfrommer C., Enßlin T. A., 2004b, *MNRAS*, 352, 76
- Pfrommer C., Enßlin T. A., Springel V., 2008, *MNRAS*, 385, 1211
- Pinzke A., Oh S. P., Pfrommer C., 2013, *MNRAS*, 435, 1061
- Pinzke A., Pfrommer C., 2010, *MNRAS*, 409, 449
- Pinzke A., Pfrommer C., Bergström L., 2011, *Phys. Rev. D*, 84, 123509
- Prokhorov D. A., Churazov E. M., 2013, *ArXiv:1309.0197*
- Reimer O., Pohl M., Sreekumar P., Mattox J. R., 2003, *ApJ*, 588, 155
- Reiprich T. H., Böhringer H., 2002, *ApJ*, 567, 716
- Riebe K. et al., 2013, *Astronomische Nachrichten*, 334, 691
- Rybicki G. B., Lightman A. P., 1979, *Radiative processes in astrophysics*
- Sarazin C. L., 1999, *ApJ*, 520, 529
- Simionescu A. et al., 2013, *ApJ*, 775, 4
- Takahashi T. et al., 2012, in *Society of Photo-Optical Instrumentation Engineers (SPIE) Conference Series*, Vol. 8443, Society of Photo-Optical Instrumentation Engineers (SPIE) Conference Series
- Thierbach M., Klein U., Wielebinski R., 2003, *A&A*, 397, 53
- Totani T., Kitayama T., 2000, *ApJ*, 545, 572
- van Weeren R. J., Brüggén M., Röttgering H. J. A., Hoeft M., Nuza S. E., Intema H. T., 2011, *A&A*, 533, A35
- Vazza F., Brüggén M., 2014, *MNRAS*, 437, 2291
- VERITAS Collaboration, 2009, *ApJL*, 706, L275
- VERITAS Collaboration, 2012, *ApJ*, 757, 123
- Voit G. M., 2005, *Reviews of Modern Physics*, 77, 207
- Waxman E., Loeb A., 2000, *ApJL*, 545, L11
- Wiener J., Oh S. P., Guo F., 2013, *MNRAS*, 434, 2209
- Wik D. R., Sarazin C. L., Finoguenov A., Baumgartner W. H., Mushotzky R. F., Okajima T., Tueller J., Clarke T. E., 2011, *ApJ*, 727, 119
- Zandanel F., Pfrommer C., Prada F., 2014a, *MNRAS*, 438, 116
- Zandanel F., Pfrommer C., Prada F., 2014b, *MNRAS*, 438, 124
- Zimmer S., Conrad J., Pinzke A., 2012, in *American Astronomical Society Meeting Abstracts*, Vol. 219, American Astronomical Society Meeting Abstracts, p. 207.01